Side-Chain Ionization States in a Potassium Channel

Kishani M. Ranatunga,* Indira H. Shrivastava,† Graham R. Smith,† and Mark S. P. Sansom†
*Biophysics Section, Blackett Laboratory, Imperial College of Science, Technology, and Medicine, London SW7 2BZ, and †Laboratory of Molecular Biophysics, Department of Biochemistry, University of Oxford, Oxford OX1 3QU, United Kingdom

ABSTRACT KcsA is a bacterial K^+ channel that is gated by pH. Continuum dielectric calculations on the crystal structure of the channel protein embedded in a low dielectric slab suggest that side chains E71 and D80 of each subunit, which lie adjacent to the selectivity filter region of the channel, form a proton-sharing pair in which E71 is neutral (protonated) and D80 is negatively charged at pH 7. When K^+ ions are introduced into the system at their crystallographic positions the pattern of proton sharing is altered. The largest perturbation is for a K^+ ion at site S3, i.e., interacting with the carbonyls of T75 and V76. The presence of multiple K^+ ions in the filter increases the probability of E71 being ionized and of D80 remaining neutral (i.e., protonated). The ionization states of the protein side chains influence the potential energy profile experienced by a K^+ ion as it is translated along the pore axis. In particular, the ionization state of the E71-D80 proton-sharing pair modulates the shape of the potential profile in the vicinity of the selectivity filter. Such reciprocal effects of ion occupancy on side-chain ionization states, and of side-chain ionization states on ion potential energy profiles will complicate molecular dynamics simulations and related studies designed to calculate ion permeation energetics.

INTRODUCTION

Ion channels are a major class of integral transmembrane proteins classically involved in the control of cell excitability. They provide gated, aqueous pores through which selected ions diffuse passively down their electrochemical gradient (Hille, 1992). Mutations in channels may result in disease (Ashcroft, 2000). It is therefore of some interest to relate the molecular structure of ion channels to their physiological function. X-ray crystallographic studies have revealed the structures of a bacterial K^+ channel KcsA (Doyle et al., 1998) and of a mechanosensitive channel (Chang et al., 1998). At the same time, spectroscopic studies have revealed aspects of channel gating (Perozo et al., 1999; Cha et al., 1999; Glauner et al., 1999; Patlak, 1999). However, the microscopic basis of their ability to effectively select ions and allow them to permeate at diffusion-like rates remains an intriguing question (Meuser et al., 1999).

Potassium channels are selective for K^+ ions over other ions and act physiologically to dampen cell excitation and to maintain the membrane potential at its resting value (Hille, 1992). Site-directed mutagenesis studies combined with electrophysiology identified residues that confer selectivity (MacKinnon and Yellen, 1990). The recent elucidation of the structure of KcsA (Doyle et al., 1998) provided the first view of a potassium channel at the molecular level. Several ions were shown to be present in the channel, supporting the view of K^+ channels as single-file, multi-ion pores (Hille, 1992). Electrophysiological characterization has shown it to be a K^+-selective channel with a conductance of 83 pS (Heginbotham et al., 1999), although the existence of multiple conductance levels has also been suggested (Meuser et al., 1999). It is gated by pH such that channel opening is favored at pH < 4 (Cuello et al., 1998). EPR studies show that the opening of the spin-labeled channel involves structural changes that increase the pore radius at the intracellular mouth of the channel (Perozo et al., 1999). Although its physiological function is as yet unknown, its strong sequence homology to other K^+ channels, particularly within the filter region, suggest that all K^+ channels share a similar structure (Yellen, 1999), although it seems likely that in Kv channels one of the two pore-lining transmembrane helices may be kinked (Kerr et al., 1996; Shrivastava et al., 2000; Camino et al., 2000; Sansom and Weinstein, 2000). Thus, KcsA provides a useful structural model with which to investigate the molecular basis of ion channel function.

The crystal structure of KcsA reveals a membrane-spanning tetramer with a narrow selectivity filter at the extracellular side and a large, hydrophobic, water-filled cavity near the center of the membrane (Fig. 1 *A*). Continuum electrostatic studies suggest that dipole moments of the short pore (P) helices, which surround the filter, are able to focus an ion within this aqueous cavity (Roux and MacKinnon, 1999). Difference electron density maps, calculated from crystals soaked in Rb^+-containing solutions, reveal the existence of multiple ion binding sites. These were included in the crystal structure (Doyle et al., 1998) as three ions within the selectivity filter and one ion in the cavity (Fig. 1 *B*).

Computational simulations enable one to explore the functional implications of molecular structures of ion channels (Sansom et al., 2000). For example, molecular dynamics (MD) simulations have been used to calculate free energy profiles along the pore of gramicidin (Roux and Karplus, 1991) and more recently to estimate the relative free energies of possible configurations of ions in the filter of KcsA (Åqvist and Luzhkov, 2000; Allen et al., 2000).

Received for publication 5 June 2000 and in final form 13 December 2000.
Address reprint requests to Dr. Mark S. P. Sansom, Laboratory of Molecular Biophysics, The Rex Richards Building, Department of Biochemistry, University of Oxford, South Parks Road, Oxford, OX1 3QU, UK. Tel.: 44-1865-275371; Fax: 44-1865-275182; E-mail: mark@biop.ox.ac.uk.

0006-3495/01/03/1210/10 $2.00

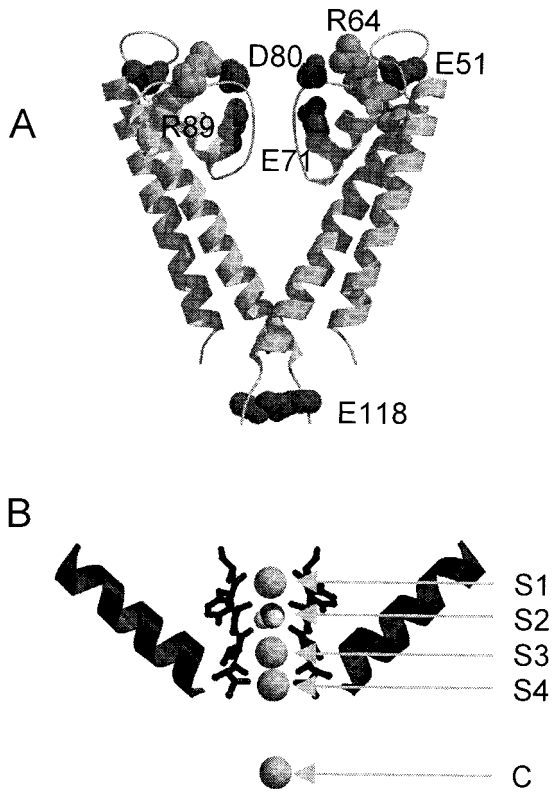

FIGURE 1 (*A*) Two subunits of the KcsA channel, viewed perpendicular to the pore axis with the extracellular mouth of the pore at the top of the diagram. Key ionizable residues are shown in space-filling format, with acidic residues in dark gray and basic residues in pale gray. (*B*) The selectivity filter region, showing two copies of the TVGYG motif and two P helices. The crystallographic locations of K^+ ions (at S1, S3, S4, and in the cavity, C) and a water molecule (at S2) are shown. Thus, S1 is at the center of the carbonyl oxygens of G77 and Y78, S2 is at the center of the carbonyl oxygens of V76 and G77, S3 is at the center of the carbonyl oxygens of T75 and V76, and S4 is formed by the carbonyl oxygens and side-chain (Oγ) oxygens of T75.

Unrestrained MD simulations of KcsA in a lipid bilayer have revealed concerted single-file motion of ions and water molecules in the filter (Shrivastava and Sansom, 2000; Bernèche and Roux, 2000). MD simulations have also been used to explore aspects of KcsA electrostatics (Guidoni et al., 1999). However, as has been shown by studies of porins (Karshikoff et al., 1994) and of simple models of ion channels (Adcock et al., 1998, 2000), the ionization states of side chains in an ion channel may differ from their default states. Such differences can have a significant effect on the energetics of ion permeation.

In this paper we present calculations of the likely ionization states of side chains of Kcs, and of how these ionization states may be modulated by the presence of K^+ ions in the filter. The protonation state of an E71-D80 pair near the selectivity filter modulates the strength of interaction of a K^+ ion with the selectivity filter.

MATERIALS AND METHODS

KcsA model

The molecular model used in this study is the x-ray crystal structure of KcsA (Protein Data Bank (PDB) file 1bl8) with the missing side chains (R27, I60, R64, E71, R117) modeled as stereochemically preferred conformers. The model omits 22 residues from the N-terminus and an additional 42 residues from the C-terminus. Each subunit of the truncated tetramer consists of two transmembrane helices (M1 and M2) connected by a ~30-amino-acid pore region consisting of a turret, a pore (P) helix, and a selectivity filter. The filter contains the highly conserved K^+ channel signature sequence TVGYG (Fig. 1).

Electrostatics calculations

The procedure for calculating pK_A values for ionizable groups in situ uses established methods (Bashford and Karplus, 1990; Yang et al., 1993), and its application to ion channel models has already been described in some detail (Adcock et al., 1998; Ranatunga et al., 1999). Similar methods have proved useful in explaining the difference in selectivity between two bacterial porins (Karshikoff et al., 1994) and yield good agreement with experimental data for bacteriorhodopsin (Bashford and Gerwert, 1992).

In brief, the calculation is based upon evaluating the change in electrostatic free energy associated with moving an isolated amino acid from an aqueous environment (in which it is characterized by an experimental model pK_A) to a protein/bilayer environment. Free energies are estimated by numerical solution of the linearized Poisson-Boltzmann equation. The energy difference in going from bulk solvent to protein/bilayer is made up of three electrostatic contributions: 1) the interaction of a side chain with the surrounding dielectric environment (i.e., the Born energy), 2) the interaction of a side chain with the background of nontitrating charges (i.e., the back energy), and 3) the interactions between the various ionizable side chains. Factors 1 and 2 combine to perturb the behavior of a side chain away from the model pK_A value to give an intrinsic pK_A. The interaction between each pair of ionizable residues when combined with the intrinsic pK_A values enables the protonation state of each individual ionizable residue to be calculated from the thermodynamic average over all possible protonation states of the protein, using

$$p(\mathbf{x}) \propto \exp\left[-\ln 10 \sum_i \gamma_i(\mathrm{pK}_{\mathrm{A,INTRINSIC},i} - \mathrm{pH}) - \beta \sum_i \sum_{k<i} \Delta G_{i,k}\right],$$

where $p(\mathbf{x})$ is the probability of a residue existing in its ionized state and $\mathbf{x}$ is an N-element state vector whose elements are 0 or 1 depending on whether the residue is un-ionized or ionized, respectively, where $\gamma = -1$ for a basic residue, $\gamma = +1$ for an acidic residue, $\beta = 1/RT$ and where $\Delta G_{i,k}$ is the screened Coulombic interaction energy between pairs of ionizable residues i and k (Bashford and Karplus, 1991; Lim et al., 1991). This procedure is carried out using a Monte-Carlo routine to minimize the computational time taken by reducing the sampling space (Smith, unpublished work; Adcock et al., 2000).

The system is represented as a mixed model of continuum solvent and microscopic protein. The lipid bilayer in which KcsA is embedded was represented by a slab of overlapping methane-sized spheres. The slab was of thickness 30 Å and centered on the channel protein. The interiors of the protein and the slab were assigned a dielectric of 4. The solvent region, both outside the channel and within its pore, was assigned a dielectric of 78 and a Debye length corresponding to an ionic strength of 100 mM. The protein atomic partial charges and radii were from the CHARMm22 set (Momany and Rone, 1992). A solvent-accessible surface of 1.4 Å and a

Stern radius of 2 Å were employed. Where ions were explicitly present, no ionic strength was included.

Molecular dynamics

Ion/protein interaction energies were evaluated via MD simulations on an ion/protein/water system using methods described in detail elsewhere (Smith and Sansom, 1997; Ranatunga et al., 1998). The system consisted of KcsA plus 2296 water molecules, the latter present within the pore and as caps at either end of the channel. This system was relaxed by a 100-ps MD simulation before analysis of ion/pore interactions. The ion was placed at successive 1-Å positions along the pore, and the nearest water molecule to the ion was removed. Harmonic restraints (force constant of 10 kcal mol^{-1} $Å^{-2}$) were applied to the *z*-position of the ion and the system minimized (3000 steps ABNR), heated (to 300 K for 6 ps), and equilibrated (9 ps). Shift functions acting between 13 and 14 Å were employed to truncate long-range interactions. Harmonic restraints were applied to the Cα atoms (see below) and an MMFP cylindrical restraint was applied to the water molecules in the caps. The potential energies of ion/protein and ion/water interactions were averaged over the 9-ps period.

Restraints

In the reduced system, which includes only protein and water and omits the bilayer, restraints are required to preserve the structural integrity of the protein. However, using a constant arbitrary restraint for all protein atoms may result in errors in estimation of protein/ion interactions (Allen et al., 1999, 2000). To mimic the motions of a channel protein in unrestrained simulations, restraints were designed to reproduce the magnitude of fluctuations observed in a 1-ns simulation of KcsA embedded in a POPC lipid bilayer (Shrivastava and Sansom, 2000). It should be noted, however, that the use of such restraints may preclude certain rare conformations that are insufficiently sampled in the original simulation.

Restraints were applied only to Cα atoms of the protein, treated as independent harmonic oscillators. The mean square value of the maximum amplitude, A, of a harmonic oscillator can be expressed in terms of the spring constant, k_S:

$$\langle A^2 \rangle = \frac{\int_0^\infty A^2 p(A) dA}{\int_0^\infty p(A) dA} = \frac{\int_0^\infty A^2 \exp[-k_S A^2/2k_B T] dA}{\int_0^\infty \exp[-k_S A^2/2k_B T] dA} = \frac{k_B T}{k_S},$$

where k_B is Boltzmann's constant, T is the temperature, and $p(A)$ is the probability distribution function of A. This was equated with the mean square fluctuation (MSF) from the average position of the Cα atoms as calculated from a full bilayer MD trajectory of KcsA (Shrivastava and Sansom, 2000) to yield a unique value for the spring constant for each Cα atom. These values were incorporated as harmonic restraints using CHARMm24, and the restrained (i.e., reduced) system was simulated for 100 ps.

The resulting restraints yield Cα MSF values closer to those from the full bilayer trajectory than did a simulation run in the absence of restraints (results not presented). To improve the quality of the restraints the spring constants were scaled by the ratio of the target MSFs (i.e., those from the full bilayer simulation) to the observed MSFs (i.e., those observed in the reduced simulation), and the restrained simulation was repeated. This procedure was iterated until a reasonable convergence was observed between the target and observed MSFs. This occurred after two consecutive scalings. These spring constants were used for all MD simulations presented in this paper.

General

All calculations were performed on either Silicon Graphics O_2 workstations or a Silicon Graphics Origin2000. All electrostatic calculations were performed using the finite-difference method with a two-step focusing protocol in UHBD5.1 (Davis et al., 1991). MD simulations used CHARMm24 (Brooks et al., 1983). Structure diagrams were drawn using Molscript (Kraulis, 1991) and Raster3D (Merritt and Bacon, 1997).

RESULTS

pK_A values of ionizable side chains

Absolute pK_A values were calculated for all 60 ionizable residues in the crystal structure of KcsA. Most of the residues remained in their default ionization states at neutral pH although their pK_A values were shifted somewhat from the corresponding model values (Table 1). However, some residues are perturbed into nonstandard ionization states, including R64 and E71.

The R64 residues have unusually low pK_A values (4.4 ± 0.3) such that they would remain neutral at pH 7. Their side chains are directed out from the top of the pore helix toward the N-termini of the neighboring M2 helices, thus forming inter-subunit interactions. Their proximity to the low dielectric of the membrane as well as unfavorable interactions with both the N-terminus of the helix dipole of M2 and the nearby R89 residues combine to lower their pK_A values (Table 1) relative to the model value of 12.0 (Nozaki and Tanford, 1967).

The intracellular mouth E118 residues form a ring in which the side chains point into the pore. They are neutral at pH 7 (Table 1) due to their close proximity to each other (~4 Å), combined with unfavorable interactions with the surrounding protein (for example, they are at the C-terminus of the M2 helix dipole). Of course, cytoplasmic regions of KcsA not present in the crystal structure may influence these residues in vivo, although we note that the channel still retains its functional properties in the absence of the C-terminal cytoplasmic region, and both regions are suggested to project away from the transmembrane domain of the protein (Perozo et al., 2000).

TABLE 1 Results of pKA calculations

Side chain	Model pK_A	Born energy (kcal mol^{-1})	Back energy (kcal mol^{-1})	Intrinsic pK_A	Absolute pK_A
H25	6.3	3.4 ± 0.1	−0.4 ± 0.1	4.1 ± 0.1	1.9 ± 0.2
R27	12.0	0.5 ± 0.0	0.7 ± 0.0	11.1 ± 0.0	11.1 ± 0.0
E51	4.4	−6.9 ± 0.1	12.3 ± 1.0	0.5 ± 0.7	<0.0
R52	12.0	3.1 ± 0.1	−1.4 ± 0.3	10.8 ± 0.2	14.5 ± 0.0
R64	12.0	2.2 ± 0.1	5.5 ± 0.3	6.4 ± 0.2	4.4 ± 0.3
E71	4.4	−6.6 ± 0.1	6.7 ± 1.1	4.4 ± 0.8	>14.5
D80	4.0	−4.1 ± 0.0	1.6 ± 1.0	5.8 ± 0.8	3.7 ± 2.2
R89	12.0	5.8 ± 0.1	1.8 ± 0.6	6.5 ± 0.4	14.5
R117	12.0	1.0 ± 0.0	−0.6 ± 0.0	11.7 ± 0.0	12.0 ± 0.0
E118	4.4	−1.8 ± 0.0	−1.7 ± 0.4	6.9 ± 0.3	10.8 ± 2.8

The pK_A calculations were performed in the absence of K^+ ions. Values given are averages (±SD) for the four copies of each residue in the channel.

E71 and D80 lie near the selectivity filter and have been suggested to interact to form a proton-sharing pair within each subunit (Bernèche and Roux, 2000). This is supported by more recent crystallographic data (Mackinnon, 2000). The side chains of E71 point upward from the bottom of the P helix near the selectivity filter (Fig. 1 *A*). The conformations of these side chains have been modeled. Their absence from the 3.2-Å-resolution crystal structure coordinates might be indicative of significant conformational flexibility. The D80 residues lie at the extracellular end of the selectivity filter and their side chains are directed away from the pore and toward the E71 side chains (Fig. 1 *A*). Both residues are in a predominantly low dielectric environment, favoring their neutral (i.e., protonated) state. However, the background charges compensate for this almost perfectly. Strong interactions between E71 and D80 residues in the same subunit (8.0 kcal mol^{-1}) and of E71 with Y78 (5.0 kcal mol^{-1}) dominate and elevate the pK_A of the E71 side chains such that they are likely to be neutral at pH 7. The pK_A values of the D80 side chains are reduced somewhat, and so these residues are ionized at pH 7. The titration curves of both groups of residues (E71 and D80; Fig. 2 *A*) are complex and markedly nonsigmoidal. In particular, as the pH is increased, the increased ionization of the D80 side chains appears to suppress ionization of the E71 side chains. However, summation of the probability of ionization of each E71-D80 pair (Fig. 2 *B*) yields sigmoidal titration curves, suggesting that each pair shares one proton rather than acting as two independent sites.

Effects of K^+ ions

K^+ channels have long been thought to be multi-ion pores (Hille, 1992). For KcsA this is supported by x-ray crystallographic results (Doyle et al., 1998) and by simulation studies (Shrivastava and Sansom, 2000; Allen et al., 2000; Åqvist and Luzhkov, 2000; Bernèche and Roux, 2000). To investigate how the presence of ions may influence the ionization state of KcsA, the absolute pK_A values were recalculated in the presence of different configurations of K^+ ions within the channel. As might be anticipated, adding K^+ ions to the channel increases the probability of ionization of acidic residues while suppressing the ionization of basic residues, and such effects are more pronounced if multiple ions are present and/or an ion is close to an ionizable side chain. The maximum pK_A shifts observed were of the order of two pH units.

The E71-D80 proton-sharing site showed very strong ion dependence (Fig. 3). Both single and multiple K^+ ions in the filter had significant effects on ionization of this region of the channel protein. To discuss these effects we will use

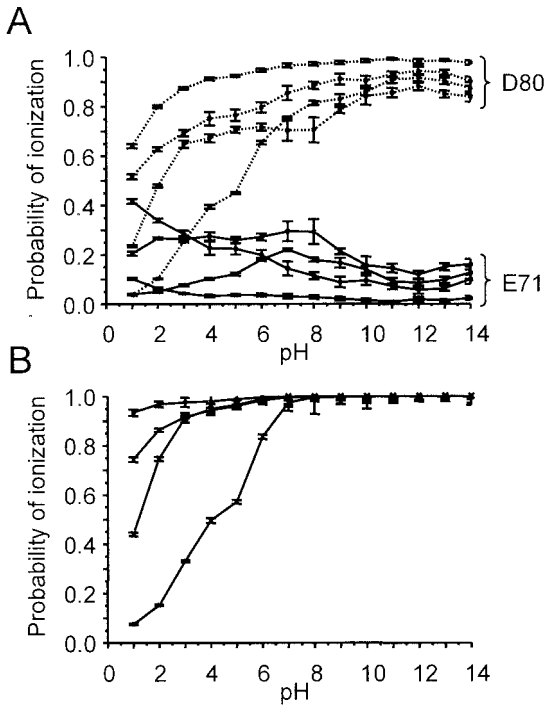

FIGURE 2 (*A*) Calculated titration curves (shown as probability of ionization versus pH) for E71 (*solid lines*) and D80 (*broken lines*) for the x-ray conformation of KcsA. (*B*) Probability of ionization of each of the four (E71, D80) pairs as a function of pH.

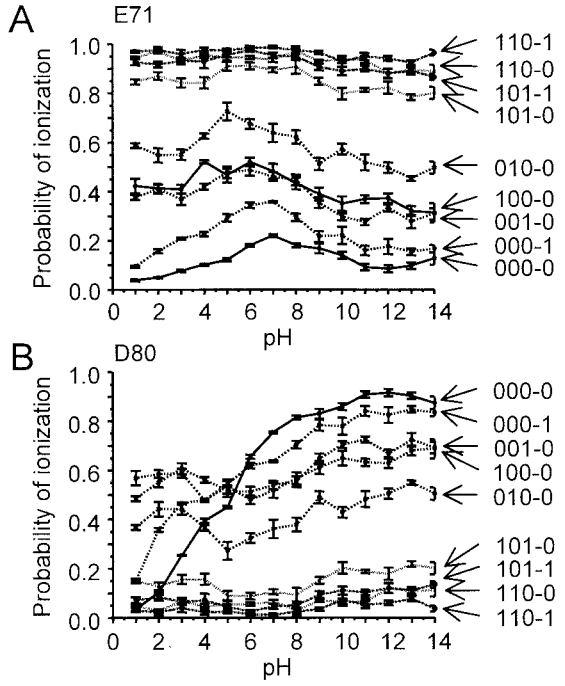

FIGURE 3 Calculated titration curves for a single E71 (*A*) and D80 (*B*) residue (from the same subunit) in the presence of different combinations of ions in the pore. The configuration of ions is indicated as follows. For sites S1, S3, S4, and the cavity C the presence/absence of an ion is indicated by a 1/0. Thus, 110–1 indicates a K^+ ion at S1, a K^+ ion at S3, and a K^+ ion in the cavity.

a nomenclature similar to that of Åqvist and Luzhkov (2000) to describe ion occupancy of the channel (see caption to Fig. 3 for details). For example, 101–1 indicates a configuration with K^+ ions at sites S1 and S4 and in the cavity (see Fig. 1 *B* for nomenclature of the K^+ ion binding sites). For a single K^+ ion present, the biggest effect on the E71-D80 pairs is obtained for configuration 010−0 (i.e., with the K^+ ion at site S3 in the middle of the filter). In contrast, if the single ion is in the cavity (configuration 000–1) the E71-D80 titration curves are not significantly different from those obtained in the absence of K^+ (i.e., 000−0). Multiple ions in the filter all have similar effects, regardless of the exact configuration. In more detail, although in the absence of ions the predominant state is E71H, $D80^-$, in the presence of multiple ions, this switches to $E71^-$, D80H. If a single ion is present in the filter (e.g., configuration 010−0), then the proton is shared equally between the two side chains. Furthermore, in the presence of multiple ions, pH has little or no effect on the ionization state of E71, D80. This suggests that the ionization state of the E71, D80 pair is unlikely to form the basis of pH gating of the channel.

Sensitivity to changes in conformation

In the context of the limited resolution of the crystallographic structure of KcsA, for which exact fourfold rotational symmetry is imposed, it is of interest to investigate the sensitivity of our pK_A calculations to small perturbations in structure. Thus, pK_A calculations were repeated for snapshots from MD simulations of KcsA in a POPC bilayer (as described in Shrivastava and Sansom, 2000). A noticeable effect of the MD simulations on this system is the loss of exact fourfold symmetry and changes in some of the networks of interactions between ionizable residues existing in the crystal structure to form new networks (Fig. 4). Note that these MD simulations were run under the assumption that all residues were all in their default ionization states. Thus, rearrangements of side chains have been driven by certain side chains moving to accommodate their fixed default charges.

Absolute pK_A values were calculated for snapshots of KcsA in a POPC bilayer simulated with no ions at 500 and 1000 ps (simulation MDK0 of Shrivastava and Sansom, 2000) and 320 ps into a simulation with three K^+ ions (simulation MDK3). The pK_A values for the structures after MD simulation (data not shown) differ from those calculated from the x-ray structure in that all of the pK_A values became consistent with the default ionization states used in the MD simulations. In effect, the unrestrained MD simulations allow residues to move to accommodate their assumed charge states. For example, the E71-D80 interaction (see above) is disrupted. The D80 side chain, instead of interacting with E71, forms intra-subunit interactions with R64 and inter-subunit interactions with R89. This is similar to the conformation in MD simulations of KcsA embedded in an octane slab (Guidoni et al., 1999)). Meanwhile, E71 interacts with the NH backbone atoms of D80 (Fig. 4 *A*).

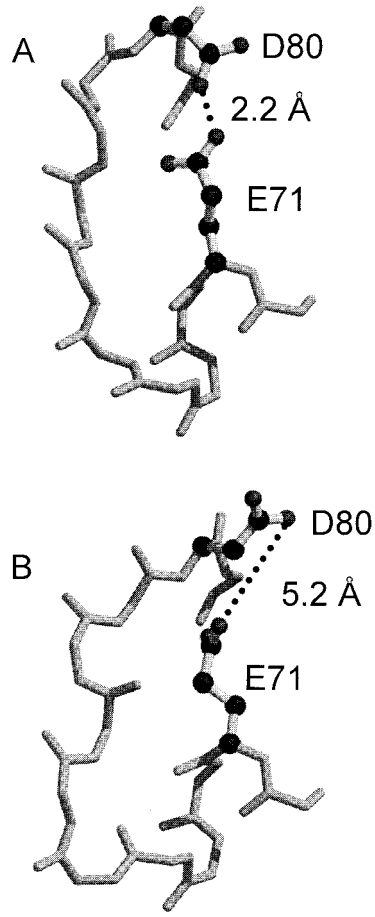

FIGURE 4 Changes in conformation of an E71, D80 pair during a bilayer MD simulation (Shrivastava and Sansom, 2000). E71, D80 pair before (*A*) and after (*B*) 0.5 ns of simulation. Note the change in the closest approach of the two side chains.

These MD simulations also generated changes in the E118 ring, the side chains of which no longer pointed in toward the pore. Instead the E118 side chains pointed away from the pore interacting with the positive ionizable groups around the intracellular mouth. This allows all the E118 residues to be ionized, but their exact pK_A values vary according to which segment the residue is in; i.e., a degree of asymmetry is seen. Furthermore, for each E118 residue, its exact pK_A varies with time. Thus, although this is perhaps a somewhat extreme example, it can be seen that the magnitude of conformational changes observed in a ~500-ps MD simulation may lead to changes in pK_A values.

Effect of ionization state on electrostatic potential profiles

Having established that ionizable side chains of KcsA exhibit complex titration properties, it is useful to examine

possible functional consequences of changes in side-chain ionization states. A first approximation to this may be obtained via calculation of the electrostatic potential profile along the pore axis, using the same Poisson-Boltzmann approximation as was used in calculation of pK_A values. This was performed on KcsA with the ionizable residues 1) in their default ionization states, 2) in their neutral states (i.e., acidic residues protonated and basic residues deprotonated), and 3) in their calculated ionization states at pH 7 (as specified in Table 1).

In all three cases the profiles (Fig. 5) show clear potential wells in agreement with the cation selectivity of the channel. The electrostatic potential profiles show some difference between ionization states particularly in the vicinity of the intracellular mouth. A deep intracellular well (~ -45 kcal mol^{-1}) is a feature of the profile when default ionization states are assumed but is absent from the other two states. This is due to the E118 ring, which helps to constrict the intracellular mouth of the pore.

The overall shapes of the profiles are similar to each other in the aqueous cavity and filter regions but show significant quantitative differences. However, the potential well generated by the filter is lower for the default than that for the other two ionization states. The shape of the profiles in this region shows that the backbone carbonyls do indeed provide a cation-attractive environment within the pore, but these continuum calculations do not allow resolution of discrete ion binding sites. The extent of ionization of the E71 ring, which we have shown to proton share with the D80 ring, strongly influences the depth of the well in the selectivity filter region. In the extracellular mouth the profiles are very similar for the different ionization sates as they approach 0 kcal mol^{-1}. The profile does not show any strong cation-attractive features in this region.

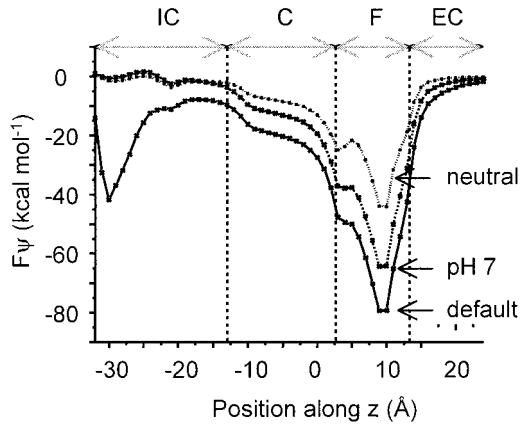

FIGURE 5 Electrostatic potential energy profiles (calculated via numerical solution of the Poisson-Boltzmann equation) along the pore axis for three different ionization states of the protein: default indicates the fully ionized state; pH 7 indicates the ionization state at pH 7 based on calculated pK_A values (Table 1); and neutral indicates that all ionizable side chains are in their uncharged state. The gray arrows above the graph indicate the approximate locations of the intracellular (IC), cavity (C), filter (F), and extracellular (EC) regions.

Effect of ionization state on potential energy of interaction with a K^+ ion

Although a continuum calculation provides an estimate of the effect of side-chain ionization on the strength of interactions of a K^+ ion with the channel, it cannot take into account, e.g., small changes in channel conformation in response to the presence of the ion or allow estimation of the relative strengths of ion/protein and ion/water interactions. To explore such aspects in a little more detail, a K^+ ion was placed at 1-Å steps along the pore axis and the potential energy of interaction was averaged during a short MD simulation. It should be noted that this provides an estimate of the effect of different ionization states on potential energies of interaction. However, the simulation times are too short to enable estimation of free energy profiles (Åqvist and Luzhkov, 2000).

First, let us examine the overall shape of the interaction profile, calculated as the interaction energy of the K^+ ion with the pore plus water (Fig. 6 *A*). A large barrier is seen at the intracellular mouth due to the narrowness of the channel here (reflected in the ion-water interaction), suggesting that the channel is in a closed conformation. This

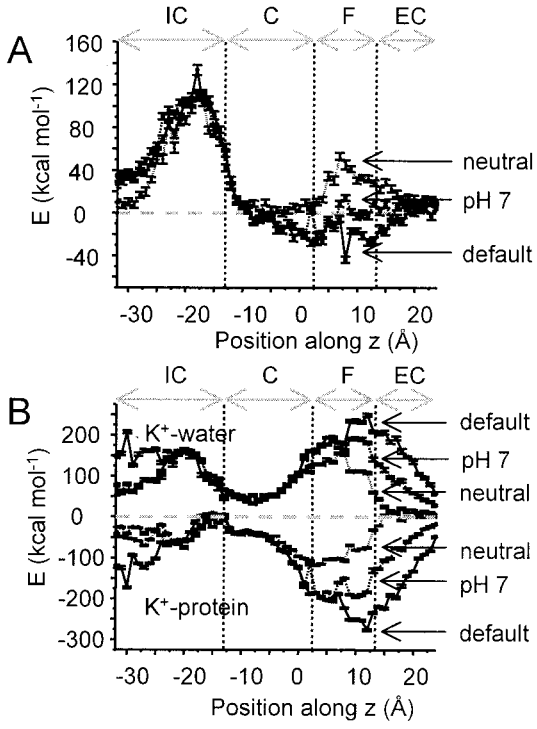

FIGURE 6 Interaction potential energy profiles for a K^+ ion as a function of position along the pore axis. (*A*) The ion-(protein + water) interaction energies; (*B*) The ion-water (*upper half*) and ion-protein (*lower half*) interaction energy profiles.

barrier is independent of the ionization state of the protein side chains. The shape of the profile in the region of cavity and filter differs markedly between different ionization states. If one assumes all side chains to be ionized (the default assumption) then there is a broad potential well, of depth ~ -40 kcal mol^{-1} in the center of the filter. If one assumes all side chains to be in their neutral state, this well is transformed to a barrier of height $\sim +50$ kcal mol^{-1}. If one takes the ionization states predicted at pH 7 using the pK_A values in Table 1, then the potential profile is much flatter, with a small well close to the cavity and a small barrier in the middle of the filter.

These profiles can be analyzed in more detail by breaking them down into ion/water and ion/protein profiles (Fig. 6 *B*). This clearly reveals that the intracellular barrier is due to an unfavorable ion/water term; i.e., the ion is desolvated as it is moved through the intracellular mouth of the (closed) channel, and even in the fully ionized system (with a ring of anionic E118 side chains), the ion/protein interactions are insufficient to compensate for this desolvation. The size and shape of this intracellular barrier vary little with ionization state except at the furthest extreme of the channel (-32 Å). This is roughly the position of the E118 ring and its positively charged neighbors (H25, R27, and R117). The principal barrier (at $z \approx -20$ Å) is due to the hydrophobic A111 and V115 rings.

Within the filter it can be seen that the ion-protein interactions are highly favorable whereas the ion-water interactions are unfavorable (relative to a fully solvated K^+ ion). The depth of the ion-protein potential well is dependent on the ionization state, ~2.5 times for the fully ionized model to ~ -100 kcal mol^{-1} for the neutral model. The latter figure is dominated by the interactions of the K^+ ion with the carbonyl oxygens that line the filter. Even in the pH 7 model, this potential well is deepened to ~ -200 kcal mol^{-1}. Thus, the state of ionization of the side chains has a strong influence on the ion-protein interaction energy profile. In particular, D80 contributes ~ -150 kcal mol^{-1} to the depth of the ion-protein well. The E71 ring, which forms a proton-sharing site with D80, is ionized only in the default state contributing ~ -120 kcal mol^{-1} to the well depth. D80 does not have a significant contribution in the pH 7 and all neutral states. Thus, even though the backbone carbonyls of the selectivity filter residues stabilize ions, the ionizable residues in the vicinity have a considerable effect on the energetics of an ion within the filter.

Of course, the final effect of these changes is seen in the ion-(protein + water) profiles. An expanded view of these within the selectivity filter is given in Fig. 7, highlighting the influence of the ionizable residues nearby (i.e., E71 and D80). The profile for the model with all neutral side chains presents a barrier of height $\sim +50$ kcal mol^{-1} in the filter, whereas both the fully ionized and pH 7 model profiles have shallow potential wells. It is informative to compare these wells with the locations of K^+ ions in the x-ray structure (at

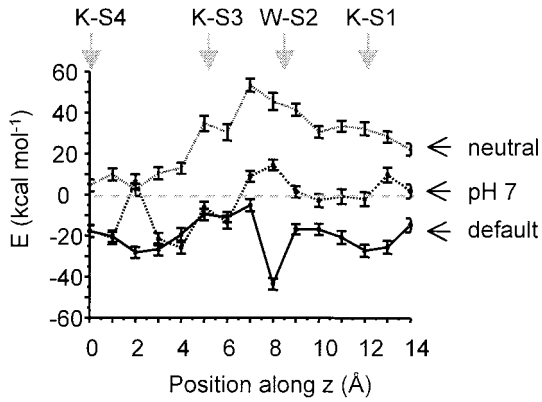

FIGURE 7 Expanded view of the K^+-(protein + water) potential energy profiles for the selectivity filter region. Profiles are shown for the same three ionization states as in Fig. 6. The vertical gray arrows show the approximate locations of the three K^+ ions and the water molecule seen in the filter in the x-ray structure.

sites S1, S3, and S4, although the latter two sites cannot be occupied simultaneously) and with the results of simulation studies (Shrivastava and Sansom, 2000; Åqvist and Luzhkov, 2000) that indicate that ions prefer to occupy sites S2 and S4. The default profile is perhaps a little more consistent with the ion occupancy in the crystal (as it has a well close to S1) whereas the pH 7 profile is perhaps closer to the simulation results. However, it should be remembered that 1) these profiles correspond to single ion occupancy and 2) simulation studies indicate that transitions between S1/S3 and S2/S4 occupancy are facile. The latter is consistent with the relatively flat profiles observed, especially for the pH 7 model.

DISCUSSION

Biological implications

The main result from this study is to demonstrate quantitatively that the most likely ionization state for several side chains in KcsA is not the default (i.e., bulk solution) ionization state for the corresponding amino acid. Although perhaps it is unsurprising in itself that pK_A values are perturbed, the degree of shifts and final pattern of protonation, due to the opposing electrostatic interactions that underlie them, can be approached only by explicit calculation. In particular, the E71-D80 pairs and the E118 ring have considerably perturbed pK_A values. It has previously been suggested, by visual examination of the structure, that the E71-D80 pair might share a single proton (Bernèche and Roux, 2000), and this suggestion is supported by the current studies. To the best of our knowledge, protonation of the E118 ring has not been suggested. These changes in ionization states of side chains from the default states are consistent with our earlier studies of models of ion channels (Adcock et al., 1998; Ranatunga et al., 1998; Adcock et al.,

2000) and add details to our picture of the molecular structure of KcsA that cannot be arrived at by x-ray diffraction. Similar shifts in pK_A values have been seen in homology models of Kv and Kir channels (based on the KcsA structure) (Capener et al., 2000; Ranatunga et al., 2001). It thus seems reasonable to conclude that such effects may be widespread in ion channels and need to be taken into account in simulations and theoretical studies.

However, there is clearly a complication in that pK_A values, if sensitive to the local protein environment, are also likely to be sensitive to changes in that local environment. For those side chains in the vicinity of the central pore running through an ion channel, a significant perturbation is likely to be the presence/absence of ions within the pore. We have explicitly shown that, in the case of KcsA, the pattern of protonation of the E71-D80 pair is sensitive to the presence/absence of K^+ ions within the selectivity filter. If no ions are present, then the degree of protonation shows some pH dependence. At pH 7 each pair shares one proton that is more likely to be on E71. If multiple K^+ ions are present within the filter, then the degree of protonation is more or less independent of pH, and the proton is more likely to be on D80. Thus, for future simulations of KcsA in the presence of ions, it is reasonable to assume that E71-D80 share a proton and that this proton is predominantly on D80.

It is important to establish the possible effects of such changes in ionization states on the function of KcsA. Previous studies of an early model of a K^+ channel pore (Ranatunga et al., 1998) suggested that changes in ionization state could alter potential energy profiles for an ion translated along the pore axis. Furthermore, it has been shown that use of predicted ionization states results in smaller drift, during an MD simulation, of a Kir channel model than was observed if default ionization states were assumed (Capener et al., 2000). In the current study we have demonstrated, by two different approaches, that changes in ionization state may have a significant effect on K^+ potential energy profiles. Although open to criticism on theoretical grounds (Moy et al., 2000), Poisson-Boltzmann calculations provide a first approximation to the electrostatic potential energy profile. Even from such approximate calculations, it is evident that changes in ionization state have an effect. These effects have been characterized in more detail by estimation of the potential energy profile for a single K^+ ion. Although absolute energy values represented must be treated with caution, it is evident that the major changes are in the shape of the profile in the selectivity filter. It will be important to estimate the effects of changes in ionization state on the relative free energies of different configurations of multiple ions within the filter (Åqvist and Luzhkov, 2000). However, even on the basis of the current calculations, it is evident that ionizable side chains that do not actually line the pore can have an effect on the energetics of ion permeation and hence on channel conductance.

We have also demonstrated that, in an unrestrained MD simulation, the side-chain conformations of KcsA seem to adjust themselves to accommodate the initial ionization states assumed. This is to be expected, but does introduce a complication into attempts to rigorously simulate ion permeation while taking into account possible changes in ionization state. Our results suggest that, even if one were to repeatedly update pK_A calculations and ionization states during a simulation, the ionization state trajectory would be somewhat sensitive to the initial ionization state of the system. This would seem to be a topic that merits further investigation.

Limitations

What are the limitations of the current study? It is evident that the pK_A results are sensitive to side-chain conformations, and so one must be cautious in over-interpreting these results. They derive from a snapshot of the channel as seen in the crystal. For example, the high temperature factors of E71 and D80 in the crystallographic model might suggest that the presence/absence of proton sharing may fluctuate with respect to time and/or between different subunits of the channel tetramer.

Furthermore, it is known that pK_A estimates are subject to errors (Antosiewicz et al., 1996; Wlodek et al., 1997; You and Bashford, 1995) associated with assuming fixed side-chain conformations during such calculations. The use of the linearized Poisson-Boltzmann equation embodies the assumption that the electrostatic energy is much less than the thermal energy of the system and has been shown to lead to errors (Jordan et al., 1989), although Weetman et al. (1997) suggest that the form of the results is unaffected by the exact method of calculation. Arguably, this assumption has already been made in approximating the potential energy of mean force with a purely electrostatic term that ignores ion-ion interactions (Daune, 1999). The Poisson-Boltzmann equation is an equilibrium treatment and has been applied to these systems in the absence of a transbilayer electrochemical gradient. Clearly, in vivo, the situation is far more complex and away from equilibrium (Chen et al., 1997). However, the very fact that ions are observed in the x-ray study would suggest that they have preferred configurations, and so an equilibrium theory may be acceptable as a first approximation. Whether these configurations can be considered as a starting point from which to consider the non-equilibrium case remains an open question and needs to be addressed in the future.

An additional possible source of error lies in the channel structure used in the calculations. It is likely that the crystal structure is closer to that of the channel in its closed state than in its open state. EPR studies (Perozo et al., 1998, 1999) suggest that the channel widens at its cytoplasmic end on opening but that little structural rearrangement occurs within the filter region of the channel. This would be

expected to change the preferred ionization state of the E118 ring but not of the E71-D80 pairs. However, it should be remembered that there are suggestions that the structure of the filter region in the open channel might differ from that in the x-ray structure (Meuser et al., 1999). Other factors to consider are that the channel structure is truncated, in that the N- and C-terminal tails of the polypeptide are absent from the x-ray structure, and that lipid headgroups have been omitted from our pK_A calculations.

Overall, these considerations indicate that further studies should be undertaken to refine our picture of the ionization states of KcsA. However, the overall conclusion remains that the true ionization state is likely to differ from the default and that this will have an effect on calculations of the energetics of ion transport. Although it might seem obvious that the presence/absence of ions and the ionization state of the channel protein will be coupled, one can only really approach an understanding of such effects via explicit, albeit approximate, calculations.

Our thanks to Rod MacKinnon and Declan Doyle for the coordinates of KcsA. Our thanks to Phil Biggin and Charlotte Adcock for useful suggestions and discussions.

This work was supported by grants from the Wellcome Trust.

REFERENCES

Adcock, C., G. R. Smith, and M. S. P. Sansom. 1998. Electrostatics and the selectivity of ligand-gated ion channels. *Biophys. J.* 75:1211–1222.

Adcock, C., G. R. Smith, and M. S. P. Sansom. 2000. The nicotinic acetylcholine receptor: from molecular model to single channel conductance. *Eur. Biophys. J.* 29:29–37.

Allen, T. W., A. Bliznyuk, A. P. Rendell, S. Kuyucak, and S. H. Chung. 2000. The potassium channel: structure, selectivity and diffusion. *J. Chem. Phys.* 112:8191–8204.

Allen, T. W., S. Kuyucak, and S. H. Chung. 1999. Molecular dynamics study of the KcsA potassium channel. *Biophys. J.* 77:2502–2516.

Antosiewicz, J., J. M. Briggs, A. H. Elcock, M. K. Gilson, and J. A. McCammon. 1996. Computing ionization states of proteins with a detailed charge model. *J. Comp. Chem.* 17:1633–1644.

Åqvist, J., and V. Luzhkov. 2000. Ion permeation mechanism of the potassium channel. *Nature.* 404:881–884.

Ashcroft, F. M. 2000. Ion Channels and Disease. Academic Press, San Diego.

Bashford, D., and K. Gerwert. 1992. Electrostatic calculation of the pK_A values of ionizable groups in bacteriorhodopsin. *J. Mol. Biol.* 224: 473–486.

Bashford, D., and M. Karplus. 1990. pKa's of ionizable groups in proteins: atomic detail from a continuum electrostatic model. *Biochemistry.* 29: 10219–10225.

Bashford, D., and M. Karplus. 1991. Multiple-site titration curves of proteins: an analysis of exact and approximate methods for their calculation. *J. Phys. Chem.* 95:9556–9561.

Bernèche, S., and B. Roux. 2000. Molecular dynamics of the KcsA K^+ channel in a bilayer membrane. *Biophys. J.* 78:2900–2917.

Brooks, B. R., R. E. Bruccoleri, B. D. Olafson, D. J. States, S. Swaminathan, and M. Karplus. 1983. CHARMM: a program for macromolecular energy, minimisation, and dynamics calculations. *J. Comp. Chem.* 4:187–217.

Camino, D. D., M. Holmgren, Y. Liu, and G. Yellen. 2000. Blocker protection in the pore of a voltage-gated K^+ channel and its structural implications. *Nature.* 403:321–325.

Capener, C. E., I. H. Shrivastava, K. M. Ranatunga, L. R. Forrest, G. R. Smith, and M. S. P. Sansom. 2000. Homology modeling and molecular dynamics simulation studies of an inward rectifier potassium channel. *Biophys. J.* 78:2929–2942.

Cha, A., G. E. Snyder, P. R. Selvin, and F. Bezanilla. 1999. Atomic scale movement of the voltage-sensing region in a potassium channel measured via spectroscopy. *Nature.* 402:809–813.

Chang, G., R. H. Spencer, A. T. Lee, M. T. Barclay, and D. C. Rees. 1998. Structure of the MscL homolog from *Mycobacterium tuberculosis*: a gated mechanosensitive ion channel. *Science.* 282:2220–2226.

Chen, D., J. Lear, and B. Eisenberg. 1997. Permeation through an open channel: Poisson-Nernst-Planck theory of a synthetic ionic channel. *Biophys. J.* 72:97–116.

Cuello, L. G., J. G. Romero, D. M. Cortes, and E. Perozo. 1998. pH-Dependent gating in the *Streptomyces lividans* K^+ channel. *Biochemistry.* 37:3229–3236.

Daune, M. 1999. Molecular Biophysics: Structures in Motion. Oxford University Press, Oxford.

Davis, M. E., J. D. Madura, B. A. Luty, and J. A. McCammon. 1991. Electrostatics and diffusion of molecules in solution: simulations with the University of Houston Brownian dynamics program. *Comput. Phys. Commun.* 62:187–197.

Doyle, D. A., J. M. Cabral, R. A. Pfuetzner, A. Kuo, J. M. Gulbis, S. L. Cohen, B. T. Cahit, and R. MacKinnon. 1998. The structure of the potassium channel: molecular basis of K^+ conduction and selectivity. *Science.* 280:69–77.

Glauner, K. S., L. M. Mannuzzau, C. S. Gandhi, and E. Y. Isacoff. 1999. Spectroscopic mapping of voltage sensor movement in the *Shaker* potassium channel. *Nature.* 402:813–817.

Guidoni, L., V. Torre, and P. Carloni. 1999. Potassium and sodium binding in the outer mouth of the K^+ channel. *Biochemistry.* 38:8599–8604.

Heginbotham, L., M. LeMasurier, L. Kolmakova-Partensky, and C. Miller. 1999. Single *Streptomyces lividans* K^+ channels: functional asymmetries and sidedness of proton activation. *J. Gen. Physiol.* 114:551–559.

Hille, B. 1992. Ionic Channels of Excitable Membranes. Sinauer Associates, Sunderland, MA.

Jordan, P. C., R. J. Bacquet, J. A. McCammon, and P. Tran. 1989. How electrolyte shielding influences the electrical potential in transmembrane ion channels. *Biophys. J.* 55:1041–1052.

Karshikoff, A., V. Spassov, S. W. Cowan, R. Ladenstein, and T. Schirmer. 1994. Electrostatic properties of two porin channels from *Escherichia coli. J. Mol. Biol.* 240:372–384.

Kerr, I. D., H. S. Son, R. Sankararamakrishnan, and M. S. P. Sansom. 1996. Molecular dynamics simulations of isolated transmembrane helices of potassium channels. *Biopolymers.* 39:503–515.

Kraulis, P. J. 1991. MOLSCRIPT: a program to produce both detailed and schematic plots of protein structures. *J. Appl. Cryst.* 24:946–950.

Lim, C., D. Bashford, and M. Karplus. 1991. Absolute pKa calculations with continuum dielectric methods. *J. Phys. Chem.* 95:5610–5620.

Mackinnon, R. 2000. Mechanism of ion conduction and selectivity in K channels. *J. Gen. Physiol.* 116:6a.

MacKinnon, R., and G. Yellen. 1990. Mutations affecting TEA blockade and ion permeation in voltage activated K^+ channels. *Science.* 250: 276–279.

Merritt, E. A., and D. J. Bacon. 1997. Raster3D: photorealistic molecular graphics. *Methods Enzymol.* 277:505–524.

Meuser, D., H. Splitt, R. Wagner, and H. Schrempf. 1999. Exploring the open pore of the potassium channel from *Steptomyces lividans. FEBS Lett.* 462:447–452.

Momany, F. A., and R. Rone. 1992. Validation of the general purpose QUANTA 3.2/CHARMm forcefield. *J. Comp. Chem.* 13:888–900.

Moy, M., B. Corry, S. Kuyucak, and S. H. Chung. 2000. Tests of continuum theories as models of ion channels. I. Poisson-Boltzmann theory versus Brownian dynamics. *Biophys. J.* 78:2349–2363.

Nozaki, Y., and C. Tanford. 1967. Examination of titration behaviour. *Methods Enzymol.* 11:715–734.

Patlak, J. B. 1999. Cooperating to unlock the voltage-dependent K channel. *J. Gen. Physiol.* 113:385–387.

Perozo, E., D. M. Cortes, and L. G. Cuello. 1998. Three-dimensional architecture and gating mechanism of a K^+ channel studied by EPR spectroscopy. *Nat. Struct. Biol.* 5:459–469.

Perozo, E., D. M. Cortes, and L. G. Cuello. 1999. Structural rearrangements underlying K^+-channel activation gating. *Science.* 285:73–78.

Perozo, E., Y. S. Liu, P. Smopornpisut, D. M. Cortes, and L. G. Cuello. 2000. A structural perspective of activation gating in K^+ channels. *J. Gen. Physiol.* 116:5a.

Ranatunga, K. M., C. Adcock, I. D. Kerr, G. R. Smith, and M. S. P. Sansom. 1999. Ion channels of biological membranes: prediction of single channel conductance. *Theor. Chem. Acc.* 101:97–102.

Ranatunga, K. R., I. D. Kerr, C. Adcock, G. R. Smith, and M. S. P. Sansom. 1998. Protein-water-ion interactions in a model of the pore domain of a potassium channel: a simulation study. *Biochim. Biophys. Acta.* 1370:1–7.

Ranatunga, K. M., G. R. Smith, R. D. Law, and M. S. P. Sansom. 2001. Electrostatics and molecular dynamics of a homology model of the *Shaker* K^+ channel pore. *Euj. Biophys. J.* In press.

Roux, B., and M. Karplus. 1991. Ion transport in a model gramicidin channel: structure and thermodynamics. *Biophys. J.* 59:961–981.

Roux, B., and R. MacKinnon. 1999. The cavity and pore helices in the KcsA K^+ channel: electrostatic stabilization of monovalent cations. *Science.* 285:100–102.

Sansom, M. S. P., I. H. Shrivastava, K. M. Ranatunga, and G. R. Smith. 2000. Simulations of ion channels: watching ions and water move. *Trends Biochem. Sci.* 25:368–374.

Sansom, M. S. P., and H. Weinstein. 2000. Hinges, swivels and switches: the role of prolines in signalling via transmembrane α-helices. *Trends Pharmacol. Sci.* 21:445–451.

Shrivastava, I. H., C. Capener, L. R. Forrest, and M. S. P. Sansom. 2000. Structure and dynamics of K^+ channel pore-lining helices: a comparative simulation study. *Biophys. J.* 78:79–92.

Shrivastava, I. H., and M. S. P. Sansom. 2000. Simulations of ion permeation through a potassium channel: molecular dynamics of KcsA in a phospholipid bilayer. *Biophys. J.* 78:557–570.

Smith, G. R., and M. S. P. Sansom. 1997. Molecular dynamics study of water and Na^+ ions in models of the pore region of the nicotinic acetylcholine receptor. *Biophys. J.* 73:1364–1381.

Weetman, P., S. Goldman, and C. G. Gray. 1997. Use of the Poisson-Boltzmann equation to estimate the electrostatic free energy barrier for dielectric models of biological ion channels. *J. Phys. Chem.* 101: 6073–6078.

Wlodek, S. T., J. Antosiewicz, and J. A. McCammon. 1997. Prediction of titration properties of structures of a protein derived from molecular dynamics trajectories. *Protein Sci.* 6:373–382.

Yang, A., M. R. Gunner, R. Sampogna, K. Sharp, and B. Honig. 1993. On the calculation of pK_As in proteins. *Proteins Struct. Funct. Genet.* 15:252–265.

Yellen, G. 1999. The bacterial K^+ channel structure and its implications for neuronal channels. *Curr. Opin. Neurobiol.* 9:267–273.

You, T. J., and D. Bashford. 1995. Conformation and hydrogen ion titration of proteins: a continuum electrostatic model with conformational flexibility. *Biophys. J.* 69:1721–1733.